

**Coiled carbon nanotube structures with supraunitary nonhexagonal to hexagonal ring ratio**

László P. Biró,\* Géza I. Márk, and Antal A. Koós

*Research Institute for Technical Physics and Materials Science, H-1525 Budapest, P.O. Box 49, Hungary*

János B.Nagy and Philippe Lambin

*Facultés Universitaires Notre Dame de la Paix, 61, Rue de Bruxelles, B-5000 Namur, Belgium*

(Received 18 June 2002; published 4 October 2002)

By assembling azulene units (fused pentagon-heptagon pairs) and hexagons, and applying specific wrapping rules to these structures resembling some recently-proposed Haeckelite structures [Terrones *et al.*, Phys. Rev. Lett. **84**, 1716 (2000)], a large variety of toroidal, coiled, screwlike, and double-helix structures can be generated. In particular, the coiling appears naturally by rolling up stripes made of heptagons, hexagons and pentagons. In the structures examined here, the ratio of nonhexagonal rings to hexagonal units varies from 4:1 to 4:3. In the coiled nanotubes produced actually by catalytic chemical vapor deposition, it is not impossible that such a high concentration of nonhexagonal units in the nanotube structure be the result of a fast kinetic leading to metastable states that cannot anneal out due to the low growth temperatures used.

DOI: 10.1103/PhysRevB.66.165405

PACS number(s): 61.46.+w, 68.37.Ef, 45.10.Db, 81.15.Gh

**I. INTRODUCTION**

Since the first observation by Iijima of multiwall carbon nanotubes (MWCNT's) a decade ago,<sup>1</sup> an explosive development has taken place in the physics and chemistry of these new materials. The three main directions envisaged right now for practical applications of carbon nanotubes are (a) nanoelectronics, (b) field emission based devices and flat panel displays, and (c) carbon nanotube reinforced composite materials. The recent months brought impressive breakthroughs towards practical applications in nanoelectronics: logic gates assembled from nanowires<sup>2</sup> and carbon nanotube based logic circuits,<sup>3</sup> and in field emission devices: the achievement of a lighting element with cylindrical geometry.<sup>4</sup>

One of the major problems in producing carbon nanotube reinforced composites, which fully exploit the very high Young's modulus of carbon nanotubes, arises from the weak interaction of the straight carbon nanotubes, either single wall carbon nanotubes (SWCNT's) or MWCNT's, with the matrix in which they are incorporated.<sup>5</sup> As a consequence, the nanotubes move in the matrix similar to a sword in the scabbard. Chemical functionalization and covalent bonding through the functional groups between the CNT and the matrix may help in the case of MWCNT's. However, in the case of SWCNT's, the large number of functional groups needed makes that the carbon network is weakened in many points, so that the excellent mechanical properties of the SWCNT's may be seriously affected. A more elegant solution could be to use coiled multiwall,<sup>6</sup> single-wall,<sup>7,8</sup> or Y-branched carbon nanotubes<sup>8-11</sup> for reinforcing composite materials. As recently shown, the mechanical properties of the multiwall coiled carbon nanotubes are comparable to those of straight MWCNT's.<sup>12</sup>

The toroidal,<sup>13</sup> coiled,<sup>14,15</sup> and Y-branched<sup>16-18</sup> carbon nanotubes were predicted theoretically soon after the discovery of the straight nanotubes. All these structures are based on the insertion of nonhexagonal (n-Hx) defects in the seamless hexagonal (Hx) network. In particular, the models of the

regular helical coils of CNT's are based on a very specific arrangement of pentagons (P) and heptagons (H) in a perfect Hx lattice.<sup>15,19</sup> If the regular arrangement is perturbed by misplacing one single n-Hx ring, the structure will not be a regular coil any more.<sup>19</sup> A general characteristic of the above coil models is that the ratio n-Hx to Hx is far less than unity. For example, in the case of a single Dunlap knee connecting (3,3) to (6,0) nanotubes with a bend of 30° (Ref. 14, Fig. 2) when the smallest possible number of Hx rings is used, the ratio n-Hx/Hx is 0.125. A torus can be built by joining together 12 such knees. C<sub>540</sub> is the smallest torus made of connected (6,0) and (3,3) segments<sup>14</sup> giving n-Hx/Hx = 0.098. Larger torus diameter can be produced by adding six rows of zig-zag and six rows of armchair hexagons to increase the distance between the knees, this will yield an even lower n-Hx/Hx ratio. The toroidal structures proposed by Ihara and co-workers contain ten pentagons and ten heptagons.<sup>13</sup> This yields a ratio of 0.125 for a C<sub>360</sub> type torus. On the experimental side, C<sub>60</sub>, the first carbon cage produced, has a much higher n-Hx/Hx ratio: 0.6. It is worth pointing out that the first MWCNT's (n-Hx/Hx tends to zero) have been observed in C<sub>60</sub>-soot,<sup>1</sup> i.e., within the same experiment carbon nanostructures with quite different n-Hx/Hx ratios can be synthesized. Later on, the conditions were optimized for the preferential production of straight CNT's.

Recently new structures have been proposed for building straight carbon nanotubes<sup>20</sup> and tori<sup>21</sup> with n-Hx/Hx ratio over unity. It is worth mentioning that Terrones and co-workers<sup>20</sup> proposed tubular structures built of only pentagonal and heptagonal rings, too. These structures are thermodynamically stable. In the present paper we examine the possibility of building regular, helically coiled carbon nanotubes with n-Hx/Hx ratio higher than unity.

**II. PLANAR CONSTRUCTIONS**

The general rule we apply throughout this paper is that the polygons, which we use in all the planar constructions, are regular ones, i.e., their edges have all the same length, and

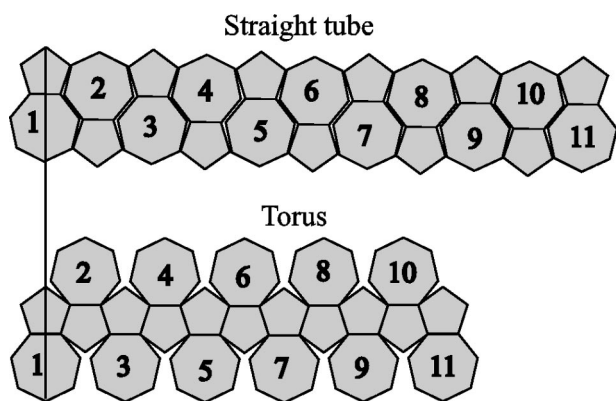


FIG. 1. Azulenoid stripes, both containing 11 units, one giving a straight tube, the other a half torus [21], respectively. The character of the generated 3D object depends on the arrangement of the polygons.

the edges of all pentagons, hexagons, and heptagons are identical.

### A. The Azulenoid stripe

When one intends to construct a planar structure which will yield a regularly coiled carbon nanotube, in some respect, this is the reverse of the task the geographers were facing when trying to map the spherical Earth onto a plane. Their solution, i.e., introducing regular cuts in the polar regions, can be adapted to the curved carbon nanostructures, too. This operation, if performed on the azulenoid torus proposed by László and Rassat,<sup>21</sup> will yield a construction similar to the one in Fig. 1. Depending on the kind of cuts used in the planar structure, the same number of “azulene” units may generate a straight tube, or a torus (actually half a torus if 11 units are used as in Fig. 1, the complete torus requires 22 azulenes). The construction is made in the following way: after closing the adjacent cuts, one atom is eliminated where two would have to occupy the same site. Then the upper edge of the crumpled sheet generated in this way is joined to the lower one, again eliminating the doubled atoms. In the case of the torus, the convex tips of the heptagons of upper (lower) edge match the concavities produced between two adjacent heptagons of the opposite edge. For the straight tube, a left or right shear has to be applied to the rolled-up structure. The structure obtained by using this latter construction remains straight, unlike the one generated from the former, which naturally circle and eventually crops itself when the number of units is large enough.

A somewhat similar construction method, yielding a truncated icosahedron, similar to the  $C_{60}$ , was proposed around the year 1500 by Dürer [Ref. 22, Fig. 1.2]. The truncated icosahedron was constructed in a similar way as discussed in Fig. 1, folding up a sheet of cardboard.

### B. The $57-1 \times 6$ stripe

The azulenoid structures discussed in the previous section are very unlikely to exist in the real world. The stress built in the C-C bond by rolling up the stripes shown in Fig. 1 to

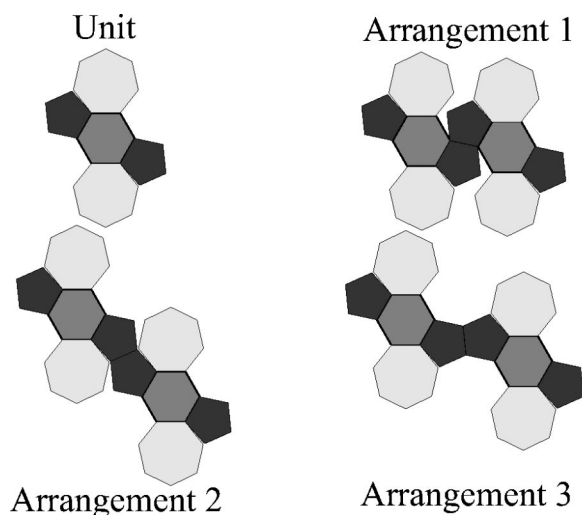


FIG. 2.  $57-1 \times 6$  unit generated from two azulene units separated by a hexagon in a way that the P, Hx, and H share common edges. Three possible ways of assembling the  $57-1 \times 6$  unit in stripes.

produce closed structures is very high due to the large curvature. To overcome this problem, one has to reduce the stress value by increasing the distance between the edges of the stripe which will be joined together, i.e., the number of polygons in a direction transversal to the stripe axis has to be increased. One way to achieve this widening of the stripe is to insert hexagons in the azulenoid structure. When a hexagon is added to an azulene-like arrangement of carbon atoms, the most compact arrangement is achieved when the P, Hx, and H rings all share common edges. The structure built according to the above rule is shown in Fig. 2. The unit of Fig. 2 can be combined in various ways to produce stripes; some of these are exemplified in the figure. In this paper we will investigate the most compact of these stripes, the arrangement labeled 1, and the further constructions that can be generated from it. The unit shown in Fig. 2 has  $n\text{-Hx}/\text{Hx}=4$ . Joining repeatedly units having the arrangement 1 yields a stripe similar to the one shown in Fig. 3. It can easily be seen that, when closing the cuts between the neighboring polygons of the stripe, a curved surface will be generated. The long edges of this surface can be joined in various ways to form closed 3D structures. These will be discussed in detail in Sec. III.

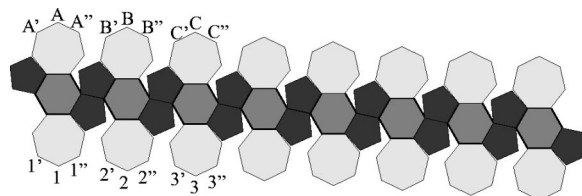


FIG. 3. Stripe of  $57-1 \times 6$  units according to the arrangement 1 from Fig. 2. The closed stripe will be generated by closing the white gaps in a way that  $A''$  will be fused with  $B'$ ,  $B''$  with  $C'$ ,  $1''$  with  $2'$ ,  $2''$  with  $3'$ , ...

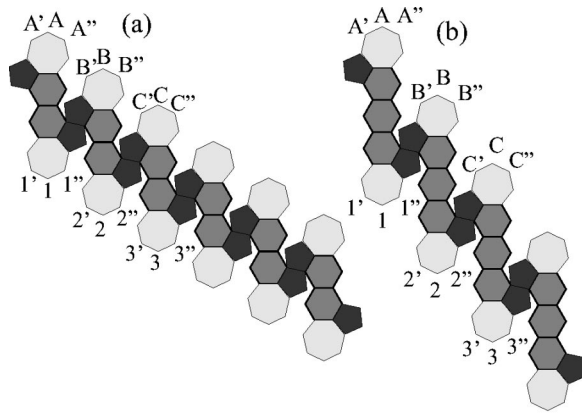


FIG. 4. Stripes  $57-2 \times 6$  and  $57-3 \times 6$  generated in a similar way as the one shown in Fig. 3. The same rules apply for obtaining a closed stripe, similar to that in Fig. 3.

### C. The $57-2 \times 6$ and the $57-3 \times 6$ stripes

The insertion of one single hexagon produces only a moderate widening of the stripe. A possible way to continue the widening in a regular way is to insert two, three, or more hexagons. The stripes generated in this way by inserting two ( $57-2 \times 6$ ) and three ( $57-3 \times 6$ ) hexagons are shown in Fig. 4. The  $n\text{-Hx}/\text{Hx}$  ratio is 2 for the stripe with two Hx, and 1.33 for the stripe with three Hx. Closing the cuts in these stripes, in a similar way as already discussed in the case of a  $57-1 \times 6$  stripe, will generate curved surfaces. These curved sheets can be closed into 3D, tubular structures of different conformations depending on the closing rules used.

## III. 3D STRUCTURES

The planar constructions shown in Figs. 3 and 4 were closed using the desktop molecular modeler (DTMM) program, the resulting construction was optimized by minimizing the bond energies. A second type of optimization was performed by minimization of the Tersoff-Brenner potential,<sup>23</sup> starting from the atomic coordinates generated by DTMM or from geometrically calculated ones. In the optimization processes, the coordination table of the atoms as defined by the starting stripe were kept fixed. The elimination of the white gaps present in the stripe  $57-1 \times 6$ , by closing side by side the neighboring polygons, as discussed above, yields closed surfaces an example of which is shown in Fig. 5. The surface in Fig. 5(a) was generated by DTMM, while the one in Fig. 5(b) was optimized with the Tersoff-Brenner potential. The two shapes are practically identical. The bowl shaped surface can be transformed into a three-dimensional (3D) closed object (neglecting the two ends) using one of the closing rules given in Table I.

It is somewhat difficult to give an unambiguous nomenclature for the resulting curved objects. The name “coil” is used for a 3D object which viewed along its coiling axis is seen as a “circle,” the name “curled tube” is used for a 3D object which viewed along its curling axis is not seen as a circle, but like an undulated line. For example the object

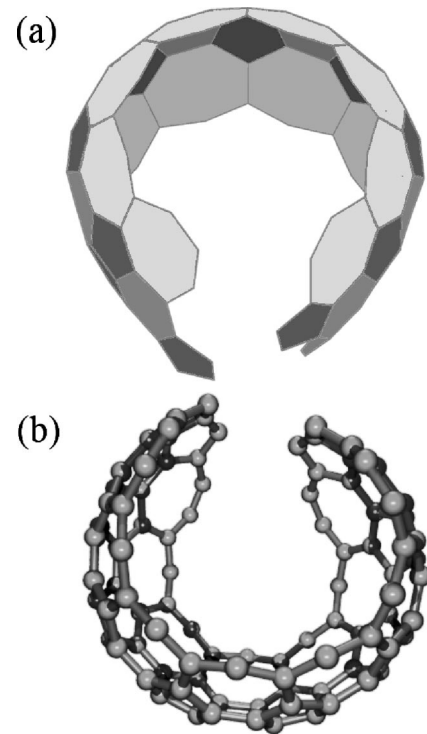


FIG. 5. Bowl-like stripes generated from the stripe of Fig. 3. (a) Structure generated with DTMM, darker shades denote the interior surface of the structure; (b) structure generated using the Tersoff-Brenner potential.

shown in Fig. 2 of Ref. 7 will be called a coil, while the

TABLE I. Closing rules used for transforming the stripes into closed 3D objects.

Stripe or sheet	Closing rule	3D structure
$57-1 \times 6$	$1'$ to $A$	Coil right hand (Fig. 6)
	$1$ to $A''$	
	$1'$ to $B$	Curled tube
	$1$ to $B''$	Curled tube
	$1'$ to $C$	
$57-2 \times 6$	$1$ to $C''$	Curled tube
	$1'$ to $A$	Coil left hand
	$1$ to $A''$	
	$1'$ to $B$	Coil right hand
	$1$ to $B''$	
$57-3 \times 6$	$1'$ to $C$	Curled tube
	$1$ to $C''$	
	$1'$ to $A$	Coil right hand [Fig. 7(a)]
	$1$ to $A''$	
	$1'$ to $B$	Curled tube
$1$ to $B''$		
$2 \times (57-1 \times 6)$	$1'(II)$ to $C(I)$	Double helix [Fig. 8(c) and 8(d)]
	$1(II)$ to $C''(I)$	

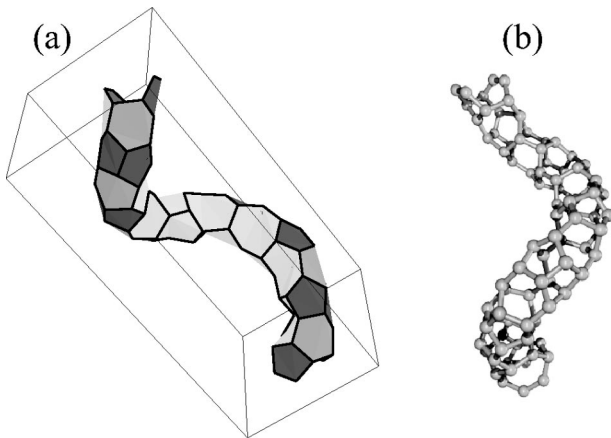


FIG. 6. Coil generated from the bowl-like surface of Fig. 5 by applying the closing rule  $1'$  to  $A$  and  $1$  to  $A''$ . (a) Coil generated with DTMM; (b) coil generated with the Tersoff-Brenner potential.

regularly undulated object seen in Fig. 1 of Ref. 24 will be called a curled tube.

When using the particular closing rule  $1'$  to  $A$ ;  $1$  to  $A''$ , for the bowl shaped objects shown in Fig. 5, one obtains a coiled tube. All other closing rules produce various curled tubes with increasing diameter as the distance between the particular edge segments (in the original planar construction polygon edges) involved in specifying the closing rule, the one denoted by letters ( $XX''$ ) and that denoted by numerals ( $n'n$ ) increases. The distance measured between these two edge segments will turn after full closing in a circle contained in the tube surface, normal to the local (coiled or curled) axis, so that the distance between the edge segments divided by  $\pi$  will give the diameter of the tube. The coiled tube obtained from the stripe  $57-1 \times 6$  using DTMM is shown in Fig. 6(a), while the coiled tube produced with the Tersoff-Brenner optimization is shown in Fig. 6(b). In a similar way one can generate coils from the stripes  $57-2 \times 6$  and the  $57-3 \times 6$ , too. The closing rules, which yield coils, are indicated in Table I. Each coil has left-handed and right-handed enantiomers.

By contrast with the earlier coil models having  $n\text{-Hx/Hx}$  ring ratios well below unity, the structure of the coils constructed here is remarkably robust. If defects are inserted, the shape of the coil suffers from minor modifications only. This is illustrated in Fig. 7 where several  $57-3 \times 6$  type coils are shown: in (a) a defect free coil, in (b) a coil in which there are carbon atoms which have only two bonding neighbors, and in (c) a structure in which these ill bonded carbons (two-fold coordinated carbons) have been fused with their regularly bonded neighbors, as a result, the hexagons were transformed in pentagons and the heptagons in hexagons in agreement with Euler's theorem for a perfect threefold coordinated network. As seen in the figure, the defects produced only a minor lengthening of the structure, while the overall shape suffered only from insignificant alterations.

It is worth mentioning that by joining several stripes, such as the ones shown in Figs. 3 and 4, one can generate sheets. These sheets are not planar like in the case of graphite. After

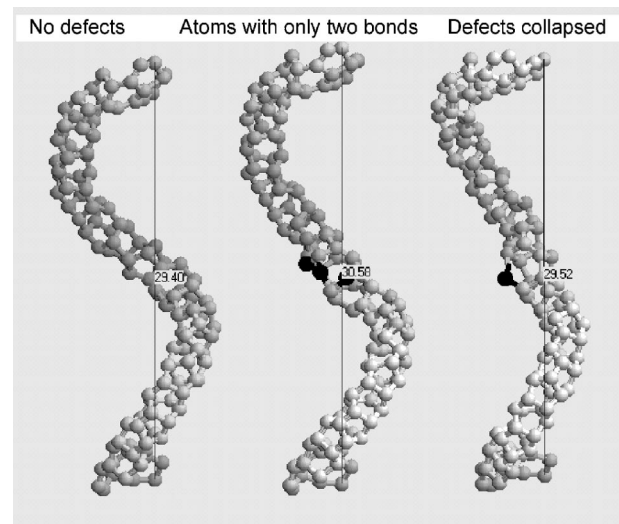


FIG. 7. Coil generated starting from a  $57-3 \times 6$  sheet using DTMM. (a) Defect free coil; (b) coil with three ill bonded carbon atoms, the ill bonded atoms are shown as dark spheres; (c) coil with the ill bonded carbon atoms fused with their neighbors. The longitudinal extension of the structures is given in Å.

optimization, the planes have a crumpled shape, such a sheet constituted of  $2 \times (8 \times [57 - 1 \times 6])$  units is shown in Fig. 8(a). On the other hand, if an average curvature is applied initially to the sheet, it rolls up and a structure resembling two fused bowls is produced, Fig. 8(b). This is not an unrealistic starting condition given that the coiled tubes are observed in catalytically grown nanotubes only. The formation of carbon rings and sheet takes place not in the free space, but nucleate on the curved surface of a catalytic particle. Generally speaking, these can be regarded as having a spherical shape, i.e., they impose an average curvature to the sheet in formation. Energy calculations for the two structures shown in Figs. 8(a) and 8(b) yield values that differ by less than 0.1 eV/atom.

Applying similar closing rules to the sheets like the ones used for the stripes, one may generate curved structures of higher complexity. In particular, using the closing rule  $1'(II)$  to  $C(I)$ ;  $1(II)$  to  $C''(I)$  where the roman numerals in brackets indicate stripe one (upper) and stripe two (lower) of the sheet composed of two stripes one may generate a regular double helix, such as the one shown in Fig. 8(c). In Fig. 8(d) an experimental, scanning tunneling microscope (STM) image is shown, in which such a double helix is seen extended over several hundreds of nanometers. If the structure would be built of two, independent, but intercoiled nanotubes, the STM topography should be different due to the particular tunneling conditions at the points where the two tubes cross each other under the STM tip. Two defect regions are indicated by white arrows, one may note that the structure has a "self-correcting" capacity, it continues defect-free growth after a short disturbed region. Similar looking double and triple helices were reported recently as being produced by iron coated indium-tin oxide catalytic particles.<sup>25</sup>

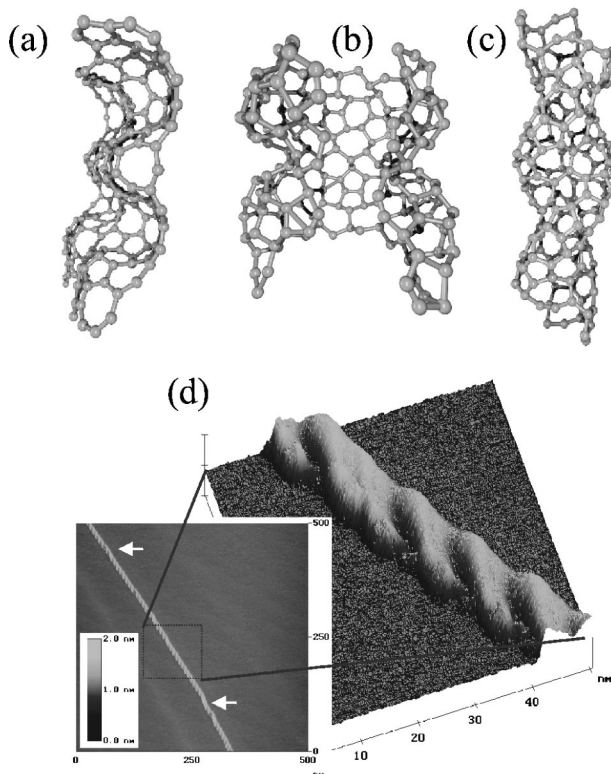


FIG. 8. Structures obtained by joining two  $57-1 \times 6$  stripes, each constituted of 8 units, similar to the arrangement 1 in Fig. 2 (two stripes shown in Fig. 3). (a) Edge view of a crumpled sheet generated by the “free” optimization of the structure; (b) two fused bowl-like structures obtained after a moderate initial curvature was imposed prior to optimization; (c) double helix type structure obtained after using a closing rule specified in the text and optimization by DTMM; (d) experimental STM image showing a double helix type structure, two defect regions are marked by white arrows. Note that before and after both of these defect regions the structure has the same periodicity.

#### IV. DISCUSSION

Nanotube coils are characteristic of low-temperature, catalytic growth methods (CVD’s). Most frequently the coiled structures are observed when using growth temperatures in the range of  $700^\circ\text{C}$ , or lower. When using high-temperature methods such as arc discharge, the product is mainly constituted of remarkably straight, well graphitized tubes, while the typical product of the CVD method consists of randomly curved tubes, or bundles of tubes in which some ordering of the curled tubes may be observed.<sup>26</sup> The random or regular curvature and the poorer graphitization of the CVD tubes as compared with the arc grown ones can be attributed to a relatively high number of n-Hx rings in the CVD structures. Regularly coiled tubes may be produced when, by accident, the growing nucleus achieves an initial n-Hx/Hx ratio and an arrangement which can generate a stable structure such as the ones described above. When comparing the cohesion energies calculated using the Tersoff-Brenner potential for graphene ( $-7.37$  eV/atom), C60 ( $-6.85$  eV/atom), and the coil shown in Fig. 6(b) ( $-6.66$  eV/atom, average over the three-fold coordinated at-

oms thus excluding the ending atoms), one may conclude that the coils built using a n-Hx/Hx ratio higher than 1 are energetically possible. In a recent paper, proposing planar sheets constituted of P, H and Hx carbon rings, and straight nanotubes generated from these — called Haeckelite tubes<sup>20</sup> — Terrones and co-workers came to the same conclusions that these straight structures built with n-Hx/Hx ratios higher than one, can be energetically more stable than C60. The bowl shaped surfaces shown in Fig. 5, if the carbon atoms having dangling bonds at the edges of the structure are not taken into account, has a bonding energy per atom of  $-7.16$  eV, not far from the value calculated for a graphene sheet. Another point worth emphasizing is that the curvature of the carbon sheet due to the incorporation of n-Hx rings may be the mechanism by which it separates from the catalytic particle — by acquiring a different curvature than that of the surface on which it started forming — and starts growing as a tube or as a coil.

Apparently, there are certain catalyst and reaction conditions, which enhance the formation of regularly coiled structures.<sup>6,12,24,25</sup> This may have to do with the formation ratio and the annealing out of n-Hx to Hx rings which could be influenced by the proper combination of growth conditions, like it was done when the Krätschmer-Huffman procedure was first optimized for MWCNT production instead of fullerene production. In particular, the annealing out of n-Hx rings may be avoided by the using of the low reaction temperatures typical for the CVD process, while the high temperatures used in the arc growth anneal out the n-Hx rings, most likely by the gliding of P-H pairs, yielding straight tubes. The epitaxial growth on the surface of the catalytic particles and templating effects may have a decisive role in achieving the selective growth of coils.

Taking into account that the helically coiled carbon nanotubes constructed with n-Hx to Hx ratio around or over 1 exhibit a remarkable structural stability with respect to defects, their stable growth can be achieved more easily than the growth of structures where after incorporating several tens of Hx rings, in a very precisely defined position P or H has to be inserted. Therefore, it is worth investigating in more detail the possible structural and electronic properties of these nanostructures as they may help explaining the existing experimental data and open the way to the understanding of the conditions under which these structures may be produced in a selective way.

#### V. CONCLUSIONS

Coiled carbon nanotubes can be produced at high yield by catalytic CVD.<sup>6,25</sup> In ideal models of these helical nanotubes, a large quantity of precisely placed pentagons and heptagons is required to bend the structure.<sup>15</sup> The problem is to explain how pentagons and heptagons can be incorporated periodically in the structure during the growth process in order to generate regular pitch and diameter of the helix. As an alternative, László and Rassat have shown that rolling up a stripe of azulenes, possibly mixed with hexagons, leads to a tube

that automatically bends and may close itself in a torus.<sup>21</sup> This construction resembles the one used to generate haeckelites nanotubes,<sup>20</sup> which contain roughly equal numbers of pentagons, hexagons, and heptagons, but remain straight cylinders. We have generalized these ideas, by assembling more complex patterns of azulenes and hexagons, and have shown that specific wrappings of these structures lead to a new variety of toroidal, coiled, screwlike, and double-helix structures. The coiling appears naturally by rolling up haeckelite-like stripes and does not demand the regular insertion of additional polygons. The structures have been shown to be robust against the presence of defects.

## ACKNOWLEDGMENTS

This work has been partly funded by the Inter-University Attraction Pole (Grant No. IUAP P5/1) on “Quantum-size effects in nanostructured materials” of the Belgian Office for Scientific, Technical, and Cultural affairs and partly by the EU5, Contracts No. NANOCOMP, HPRN-CT-2000-00037 and EU5 Center of Excellence ICAI-CT-2000-70029, and by OTKA Grants T 30435 Hungary. Two of us (L.P.B. and G.I.M.) gratefully acknowledge the Belgian Fonds National de la Recherche Scientifique and the Hungarian Academy of Sciences for financial support.

\*Electronic address: biro@mfa.kfki.hu; homepage: <http://www.mfa.kfki.hu/int/nano/>

<sup>1</sup>S. Iijima, *Nature (London)* **354**, 56 (1991).

<sup>2</sup>Y. Huang, X. Duan, Y. Cui, L.J. Lauhon, K.-H. Kim, and C.M. Lieber, *Science* **294**, 1313 (2001).

<sup>3</sup>A. Bachtold, P. Hadley, T. Nakanishi, and C. Dekker, *Science* **294**, 1317 (2001).

<sup>4</sup>J.-M. Bonard, T. Stockli, O. Noury, and A. Chatelain, *Appl. Phys. Lett.* **78**, 2775 (2001).

<sup>5</sup>L.S. Schadler, S.C. Giannaris, and P.M. Ajayan, *Appl. Phys. Lett.* **73**, 3842 (1998).

<sup>6</sup>S. Amelinckx, X.B. Zhang, D. Bernaerts, X.F. Zhang, V. Ivanov, and J.B. Nagy, *Science* **265**, 635 (1994).

<sup>7</sup>L.P. Biró, S.D. Lazarescu, P.A. Thiry, A. Fonseca, J.B. Nagy, A.A. Lucas, and P. Lambin, *Europhys. Lett.* **50**, 494 (2000).

<sup>8</sup>L.P. Biró, R. Ehlich, Z. Osváth, A. Koós, Z.E. Horváth, J. Gyulai, and J.B. Nagy, *Mater. Sci. Eng.* **19**, 3 (2002).

<sup>9</sup>J. Li, C. Papadopoulos, and J.M. Xu, *Nature (London)* **402**, 253 (1999).

<sup>10</sup>P. Nagy, R. Ehlich, L.P. Biró, and J. Gyulai, *Appl. Phys. A: Mater. Sci. Process.* **70**, 481 (2000).

<sup>11</sup>B.C. Satishkumar, P.J. Thomas, A. Govindaraj, and C.N.R. Rao, *Appl. Phys. Lett.* **77**, 2530 (2000).

<sup>12</sup>A. Volodin, M. Ahlskog, E. Seynaeve, C.V. Haesendonck, A. Fon-

seca, and J.B. Nagy, *Phys. Rev. Lett.* **84**, 3342 (2000).

<sup>13</sup>S. Ihara, S. Itoh, and J.-I. Kitakami, *Phys. Rev. B* **47**, 12 908 (1993).

<sup>14</sup>B.I. Dunlap, *Phys. Rev. B* **46**, 1933 (1992).

<sup>15</sup>S. Ihara, S. Itoh, and J. Kitakami, *Phys. Rev. B* **48**, 5643 (1993).

<sup>16</sup>A.L. Macky and H. Terrones, *Nature (London)* **352**, 762 (1991).

<sup>17</sup>G.E. Scuseria, *Chem. Phys. Lett.* **195**, 534 (1992).

<sup>18</sup>L.A. Chernozatonskii, *Phys. Lett. A* **172**, 173 (1992).

<sup>19</sup>B.I. Dunlap, *Phys. Rev. B* **49**, 5643 (1994).

<sup>20</sup>H. Terrones, M. Terrones, E. Hernández, N. Grobert, J.-C. Charlier, and P.M. Ajayan, *Phys. Rev. Lett.* **84**, 1716 (2000).

<sup>21</sup>I. László and A. Rassat, *Int. J. Quant. Chem.* **84**, 136 (2001).

<sup>22</sup>M. S. Dresselhaus, G. Dresselhaus, and P. C. Eklund, *Science of Fullerenes and Carbon Nanostructures* (Academic Press, San Diego, 1996), p. 2.

<sup>23</sup>D. Brenner, *Phys. Rev. B* **42**, 9458 (1990).

<sup>24</sup>X. Wang, Z. Hu, Q. Wu, X. Chen, and Y. Chen, *Thin Solid Films* **390**, 130 (2001).

<sup>25</sup>M. Zhang, Y. Nakayama, and L. Pan, *J. Appl. Phys.* **39**, L1442 (2000).

<sup>26</sup>J.-F. Colomer, P. Piedigrosso, K. Mukhopadhyay, Z. Kónya, I. Willems, A. Fonseca, and J. B. Nagy, in *Recent Advances in the Chemistry of Fullerenes and Related Materials*, edited by K. M. Kadish and R. S. Ruoff (The Electrochemical Society, Pennington, NJ, 1998), Vol. 98-8, p. 830.